METHODS

No statistical methods were used to predetermine sample size. The experiments were not randomized and the investigators were not blinded to allocation during experiments and outcome assessment.

Ancient DNA analysis. We screened skeletal samples for DNA preservation in dedicated clean rooms. We extracted DNA[34–36] and prepared barcoded next-generation sequencing libraries, the majority of which were treated with uracil-DNA glycosylase (UDG) to greatly reduce the damage (except at the terminal nucleotide) that is characteristic of ancient DNA[37,38] (Supplementary Information section 4). We initially enriched libraries for sequences overlapping the mitochondrial genome[39] and approximately 3,000 nuclear SNPs, using synthesized baits (CustomArray) that we PCR-amplified. We sequenced the enriched material on an Illumina NextSeq instrument with 2×76 cycles, and 2×7 cycles to read out the two indices[40]. We merged read pairs with the expected barcodes that overlapped by at least 15 bases, mapped the merged sequences to the human reference genome hg19 and to the reconstructed mitochondrial DNA consensus sequence[41] using the 'samse' command in bwa v.0.6.1[42], and then removed duplicated sequences. We evaluated DNA authenticity by estimating the rate of mismatching to the consensus mitochondrial sequence[43], and also by requiring that the rate of damage at the terminal nucleotide was at least 3% for UDG-treated libraries[43] and 10% for non-UDG-treated libraries[44].

For libraries that appeared promising after screening, we enriched in two consecutive rounds for sequences overlapping 1,233,013 SNPs ('1,240k SNP capture')[2,10] and sequenced 2×76 cycles and 2×7 cycles on an Illumina NextSeq500 instrument. We bioinformatically processed the data in the same way as for the mitochondrial capture data, except that this time we mapped only to hg19 and merged the data from different libraries of the same individual. We further evaluated authenticity by looking at the ratio of X-to-Y chromosome reads and estimating X-chromosome contamination in males based on the rate of heterozygosity[45]. Samples with evidence of contamination were either filtered out or restricted to sequences with terminal cytosine deamination in order to remove sequences that derived from modern contaminants. Finally, we filtered out samples with fewer than 10,000 targeted SNPs covered at least once and samples that were first-degree relatives of others in the dataset (keeping the sample with the larger number of covered SNPs) (Supplementary Table 1) from our genome-wide analysis dataset.

Mitochondrial haplogroup determination. We used the mitochondrial capture .bam files to determine the mitochondrial haplogroup of each sample with new data, restricting our analysis to sequences with MAPQ ≥ 30 and base quality ≥ 30. First, we constructed a consensus sequence with samtools and bcftools[46], using a majority rule and requiring a minimum coverage of two. We called haplogroups with HaploGrep2[47] based on phylotree[48] (mtDNA tree build 17 (accessed 18 February 2016)). Mutational differences, compared to the revised Cambridge Reference Sequence (GenBank reference sequence: NC_012920.1) and corresponding haplogroups, can be viewed in Supplementary Table 2. We computed haplogroup frequencies for relevant ancient populations (Supplementary Table 3) after removing close relatives with the same mtDNA.

Y-chromosome analysis. We determined Y-chromosome haplogroups for both new and published samples (Supplementary Information section 5). We made use of the sequences mapping to 1,240k Y-chromosome targets, restricting our analysis to sequences with mapping quality ≥ 30 and bases with quality ≥ 30. We called haplogroups by determining the most derived mutation for each sample, using the nomenclature of the International Society of Genetic Genealogy (http://www.isogg.org) version 11.110 (accessed 21 April 2016). Haplogroups and their supporting derived mutations can be viewed in Supplementary Table 4.

Merging newly generated data with published data. We assembled two datasets for genome-wide analyses. The first dataset is HO, which includes 2,572 present-day individuals from worldwide populations genotyped on the Human Origins Array[11,12,49] and 683 ancient individuals. The ancient set includes 211 Beaker-complex-associated individuals (195 newly reported, 7 with shotgun data[3] for which we generated 1,240k capture data and 9 that had previously been published[3,4]), 68 newly reported individuals from relevant ancient populations and 298 individuals that had previously been published[12,18,19,21–23,50–57] (Supplementary Table 1). We kept 591,642 autosomal SNPs after intersecting autosomal SNPs in the 1,240k capture with the analysis set of 594,924 SNPs from a previous publication[11]. The second dataset is HOIll, which includes the same set of ancient samples and 300 present-day individuals from 142 populations sequenced to high coverage as part of the Simons Genome Diversity Project[13]. For this dataset, we used 1,054,671 autosomal SNPs, excluding SNPs of the 1,240k array located on sex chromosomes or with known functional effects.

For each individual, we represented the allele at each SNP by randomly sampling one sequence and discarding the first and the last two nucleotides of each sequence.

Abbreviations. We have used the following abbreviations in population labels: E, Early; M, Middle; L, Late; N, Neolithic; CA, Copper Age; BA, Bronze Age; BC, Beaker complex; N_Iberia, northern Iberia; C_Iberia, central Iberia; SE_Iberia, southeast Iberia; and SW_Iberia, southwest Iberia.

Principal component analysis. We carried out principal component analysis on the HO dataset using the 'smartpca' program in EIGENSOFT[58]. We computed principal components on 990 present-day west Eurasians and projected ancient individuals using lsqproject:YES and shrinkmode:YES.

ADMIXTURE analysis. We performed model-based clustering analysis using ADMIXTURE[17] on the HO reference dataset, which included 2,572 present-day individuals from worldwide populations and the ancient individuals. First, we carried out linkage disequilibrium pruning on the dataset using PLINK[59] with the flag–indep-pairwise 200 25 0.4, leaving 306,393 SNPs. We ran ADMIXTURE with the cross validation (–cv.) flag specifying from $K=2$ to $K=20$ clusters, with 20 replicates for each value of K. For each value of K, the replicate with highest log likelihood was kept. In Extended Data Fig. 3b we show the cluster assignments at $K=8$ of newly reported individuals and other relevant ancient samples for comparison. We chose this value of K as it was the lowest one for which components of ancestry related both to Iranian Neolithic farmers and European Mesolithic hunter-gatherers were maximized.

***f*-statistics.** We computed f-statistics on the HOIll dataset using ADMIXTOOLS[49] with default parameters (Supplementary Information section 6). We used qpDstat with f4mode:Yes for f_4-statistics and qp3Pop for outgroup f_3-statistics. We computed standard errors using a weighted block jackknife[60] over 5-Mb blocks.

Inference of mixture proportions. We estimated ancestry proportions on the HOIll dataset using qpAdm[2] and a basic set of nine outgroups: Mota, Ust_Ishim, MA1, Villabruna, Mbuti, Papuan, Onge, Han and Karitiana. For some analyses (Supplementary Information section 8) we added additional outgroups to this basic set.

Admixture graph modelling. We modelled the relationships between populations in an Admixture Graph framework with the software qpGraph in ADMIXTOOLS[49], using the HOIll dataset and Mbuti as an outgroup (Supplementary Information section 7).

Allele frequency estimation from read counts. We used allele counts at each SNP to perform maximum likelihood estimations of allele frequencies in ancient populations as in ref. 4. In Extended Data Fig. 7, we show derived allele frequency estimates at three SNPs of functional importance for different ancient populations.

Data availability. All 1,240k and mitochondrial capture sequencing data are available from the European Nucleotide Archive, accession number PRJEB23635. The genotype dataset is available from the Reich Laboratory website at https://reich.hms.harvard.edu/datasets.

34. Dabney, J. *et al.* Complete mitochondrial genome sequence of a Middle Pleistocene cave bear reconstructed from ultrashort DNA fragments. *Proc. Natl Acad. Sci. USA* **110,** 15758–15763 (2013).
35. Damgaard, P. B. *et al.* Improving access to endogenous DNA in ancient bones and teeth. *Sci. Rep.* **5,** 11184 (2015).
36. Korlević, P. *et al.* Reducing microbial and human contamination in DNA extractions from ancient bones and teeth. *Biotechniques* **59,** 87–93 (2015).
37. Rohland, N., Harney, E., Mallick, S., Nordenfelt, S. & Reich, D. Partial uracil–DNA–glycosylase treatment for screening of ancient DNA. *Philos. Trans. R. Soc. Lond. B* **370,** 20130624 (2015).
38. Briggs, A. W. *et al.* Removal of deaminated cytosines and detection of *in vivo* methylation in ancient DNA. *Nucleic Acids Res.* **38,** e87 (2010).
39. Maricic, T., Whitten, M. & Pääbo, S. Multiplexed DNA sequence capture of mitochondrial genomes using PCR products. *PLoS ONE* **5,** e14004 (2010).
40. Kircher, M., Sawyer, S. & Meyer, M. Double indexing overcomes inaccuracies in multiplex sequencing on the Illumina platform. *Nucleic Acids Res.* **40,** e3 (2012).
41. Behar, D. M. *et al.* A 'Copernican' reassessment of the human mitochondrial DNA tree from its root. *Am. J. Hum. Genet.* **90,** 675–684 (2012).
42. Li, H. & Durbin, R. Fast and accurate short read alignment with Burrows–Wheeler transform. *Bioinformatics* **25,** 1754–1760 (2009).
43. Fu, Q. *et al.* A revised timescale for human evolution based on ancient mitochondrial genomes. *Curr. Biol.* **23,** 553–559 (2013).
44. Sawyer, S., Krause, J., Guschanski, K., Savolainen, V. & Pääbo, S. Temporal patterns of nucleotide misincorporations and DNA fragmentation in ancient DNA. *PLoS ONE* **7,** e34131 (2012).
45. Korneliussen, T. S., Albrechtsen, A. & Nielsen, R. ANGSD: analysis of next generation sequencing data. *BMC Bioinformatics* **15,** 356 (2014).
46. Li, H. *et al.* The sequence alignment/map format and SAMtools. *Bioinformatics* **25,** 2078–2079 (2009).
47. Weissensteiner, H. *et al.* HaploGrep 2: mitochondrial haplogroup classification in the era of high-throughput sequencing. *Nucleic Acids Res.* **44,** W58–W63 (2016).

48. van Oven, M. & Kayser, M. Updated comprehensive phylogenetic tree of global human mitochondrial DNA variation. *Hum. Mutat.* **30,** E386–E394 (2009).
49. Patterson, N. *et al.* Ancient admixture in human history. *Genetics* **192,** 1065–1093 (2012).
50. Raghavan, M. *et al.* Upper Palaeolithic Siberian genome reveals dual ancestry of Native Americans. *Nature* **505,** 87–91 (2014).
51. Omrak, A. *et al.* Genomic evidence establishes Anatolia as the source of the European Neolithic gene pool. *Curr. Biol.* **26,** 270–275 (2016).
52. Gallego Llorente, M. *et al.* Ancient Ethiopian genome reveals extensive Eurasian admixture in Eastern Africa. *Science* **350,** 820–822 (2015).
53. Fu, Q. *et al.* The genetic history of Ice Age Europe. *Nature* **534,** 200–205 (2016).
54. Kılınç, G. M. *et al.* The demographic development of the first farmers in Anatolia. *Curr. Biol.* **26,** 2659–2666 (2016).
55. Gallego-Llorente, M. *et al.* The genetics of an early Neolithic pastoralist from the Zagros, Iran. *Sci. Rep.* **6,** 31326 (2016).
56. Olalde, I. *et al.* Derived immune and ancestral pigmentation alleles in a 7,000-year-old Mesolithic European. *Nature* **507,** 225–228 (2014).
57. Hofmanová, Z. *et al.* Early farmers from across Europe directly descended from Neolithic Aegeans. *Proc. Natl Acad. Sci. USA* **113,** 6886–6891 (2016).
58. Patterson, N., Price, A. L. & Reich, D. Population structure and eigenanalysis. *PLoS Genet.* **2,** e190 (2006).
59. Purcell, S. *et al.* PLINK: a tool set for whole-genome association and population-based linkage analyses. *Am. J. Hum. Genet.* **81,** 559–575 (2007).
60. Busing, F. M. T. A., Meijer, E. & Van Der Leeden, R. Delete-m jackknife for unequal m. *Stat. Comput.* **9,** 3–8 (1999).
61. Rojo-Guerra, M. Á., Kunst, M., Garrido-Pena, R. & García-Martínez de Lagrán, I. & Morán-Dauchez, G. *Un desafío a la eternidad. Tumbas monumentales del Valle de Ambrona (Memorias Arqueología en Castilla y León 14)* (Junta de Castilla y León, 2005).
62. Gamba, C. *et al.* Genome flux and stasis in a five millennium transect of European prehistory. *Nat. Commun.* **5,** 5257 (2014).

Extended Data Figure 1 | Beaker-complex artefacts. a, 'All-Over-Cord' Beaker from Bathgate, West Lothian, Scotland. Photograph: © National Museums Scotland. **b**, Beaker-complex grave goods from La Sima III barrow, Soria, Spain[61]. The set includes Beaker pots of the so-called 'Maritime style'. Photograph: Junta de Castilla y León, Archivo Museo Numantino, Alejandro Plaza.

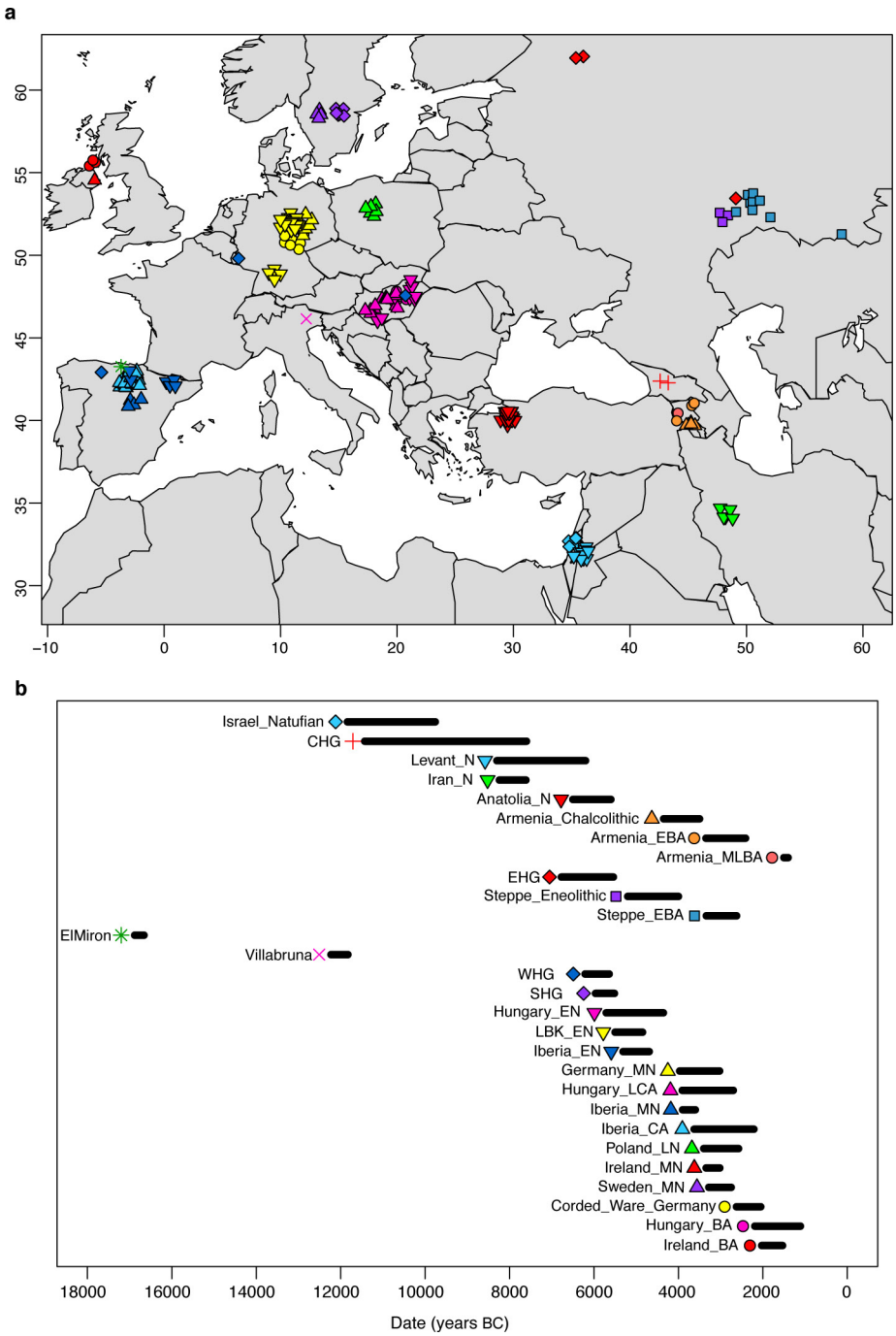

Extended Data Figure 2 | Ancient individuals with previously published genome-wide data used in this study. a, Sampling locations. **b**, Time ranges. WHG, western hunter-gatherers; EHG, eastern hunter-gatherers; SHG, Scandinavian hunter-gatherers; CHG, Caucasus hunter-gatherers; E, Early; M, Middle; L, Late; N, Neolithic; CA, Copper Age; and BA, Bronze Age. Map data from the R package 'maps'.

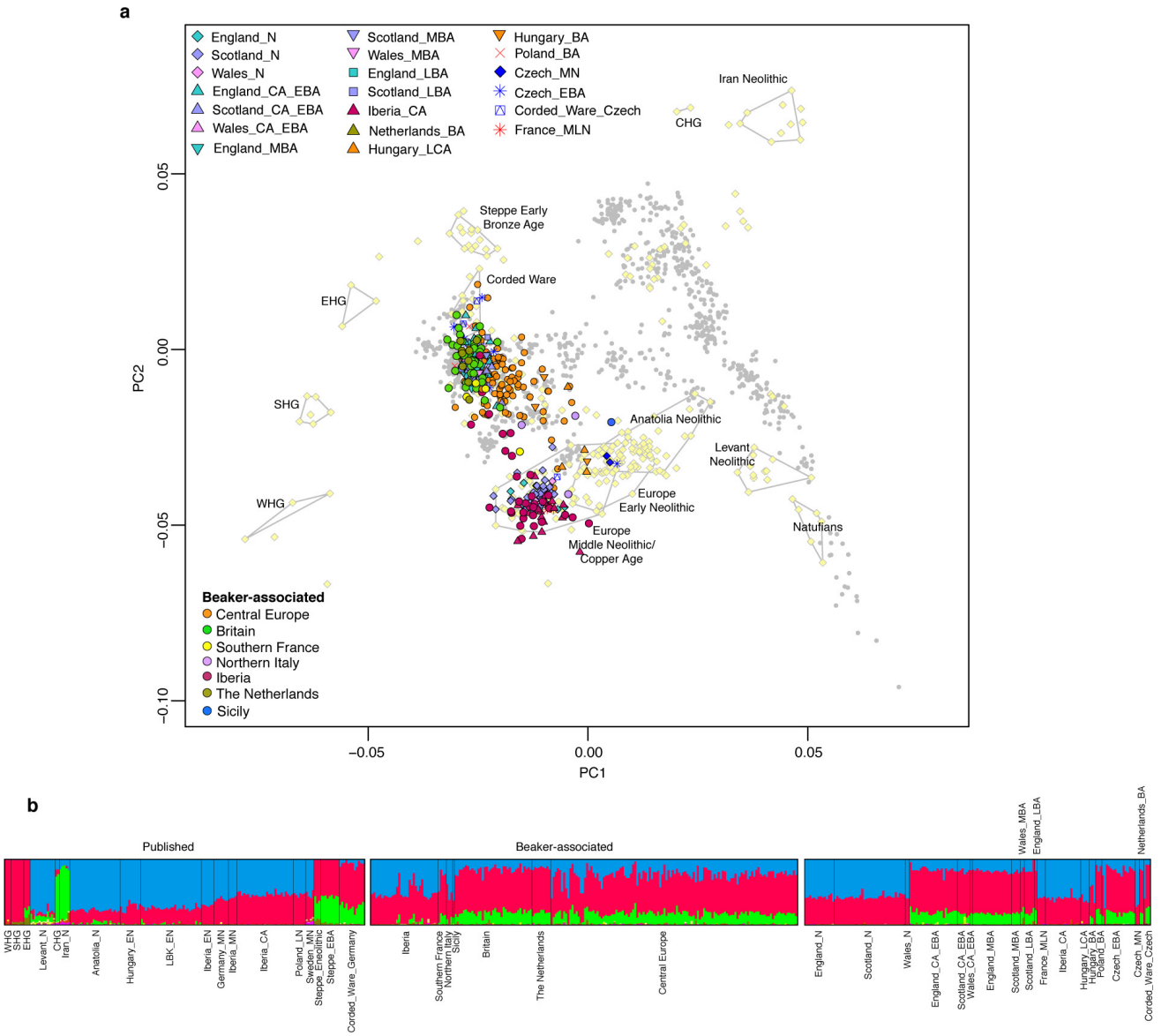

Extended Data Figure 3 | Population structure. a, Principal component analysis of 990 present-day west Eurasian individuals (grey dots), with previously published (pale yellow) and new ancient samples projected onto the first two principal components. **b**, ADMIXTURE clustering analysis with $K = 8$ showing ancient individuals. WHG, western hunter-gatherers; EHG, eastern hunter-gatherers; SHG, Scandinavian hunter-gatherers; CHG, Caucasus hunter-gatherers; E, Early; M, Middle; L, Late; N, Neolithic; CA, Copper Age; and BA, Bronze Age.

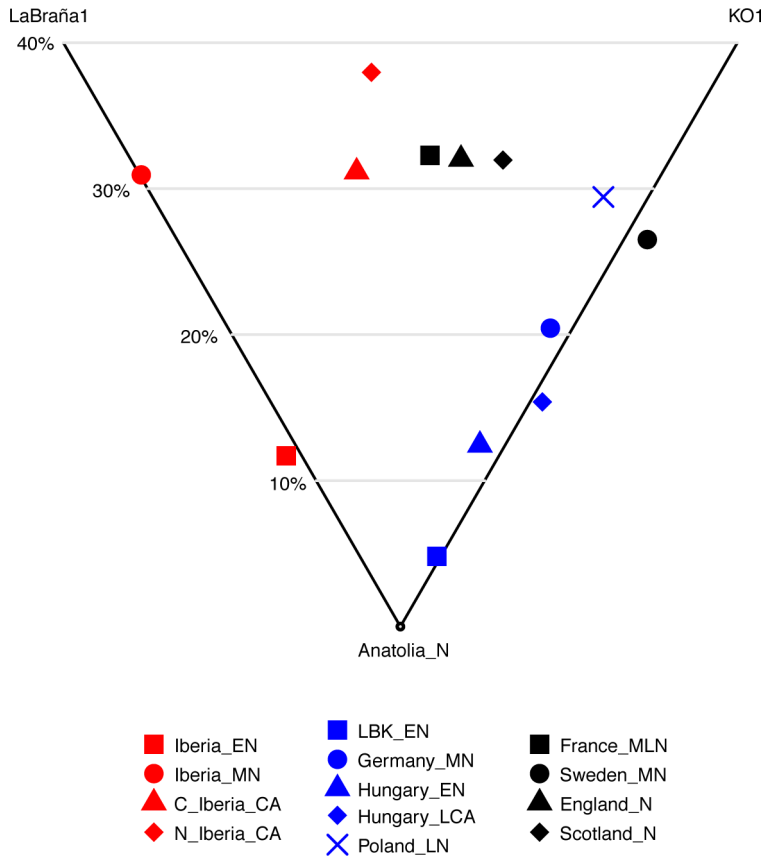

Extended Data Figure 4 | Hunter-gatherer affinities in Neolithic and Copper Age Europe. Differential affinity to hunter-gatherer individuals (La Braña1[56] from Spain and KO1[62] from Hungary) in European populations before the emergence of the Beaker complex. See Supplementary Information section 8 for mixture proportions and standard errors computed with qpAdm[2]. E, Early; M, Middle; L, Late; N, Neolithic; CA, Copper Age; BA, Bronze Age; N_Iberia, northern Iberia; and C_Iberia, central Iberia.

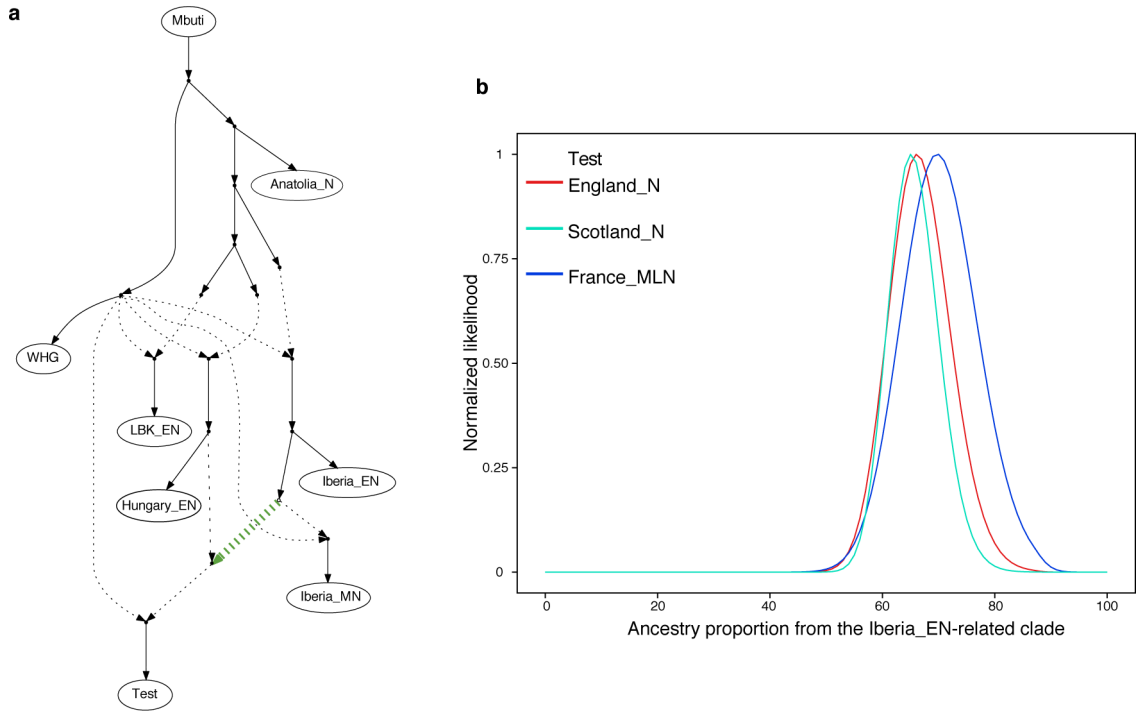

Extended Data Figure 5 | Modelling the relationships between Neolithic populations. a, Admixture graph fitting a test population as a mixture of sources related to both Iberia_EN and Hungary_EN. **b**, Likelihood distribution for models with different proportions of the source related to Iberia_EN (green admixture edge in **a**) when the test population is England_N, Scotland_N or France_MLN. E, Early; M, Middle; L, Late; and N, Neolithic.

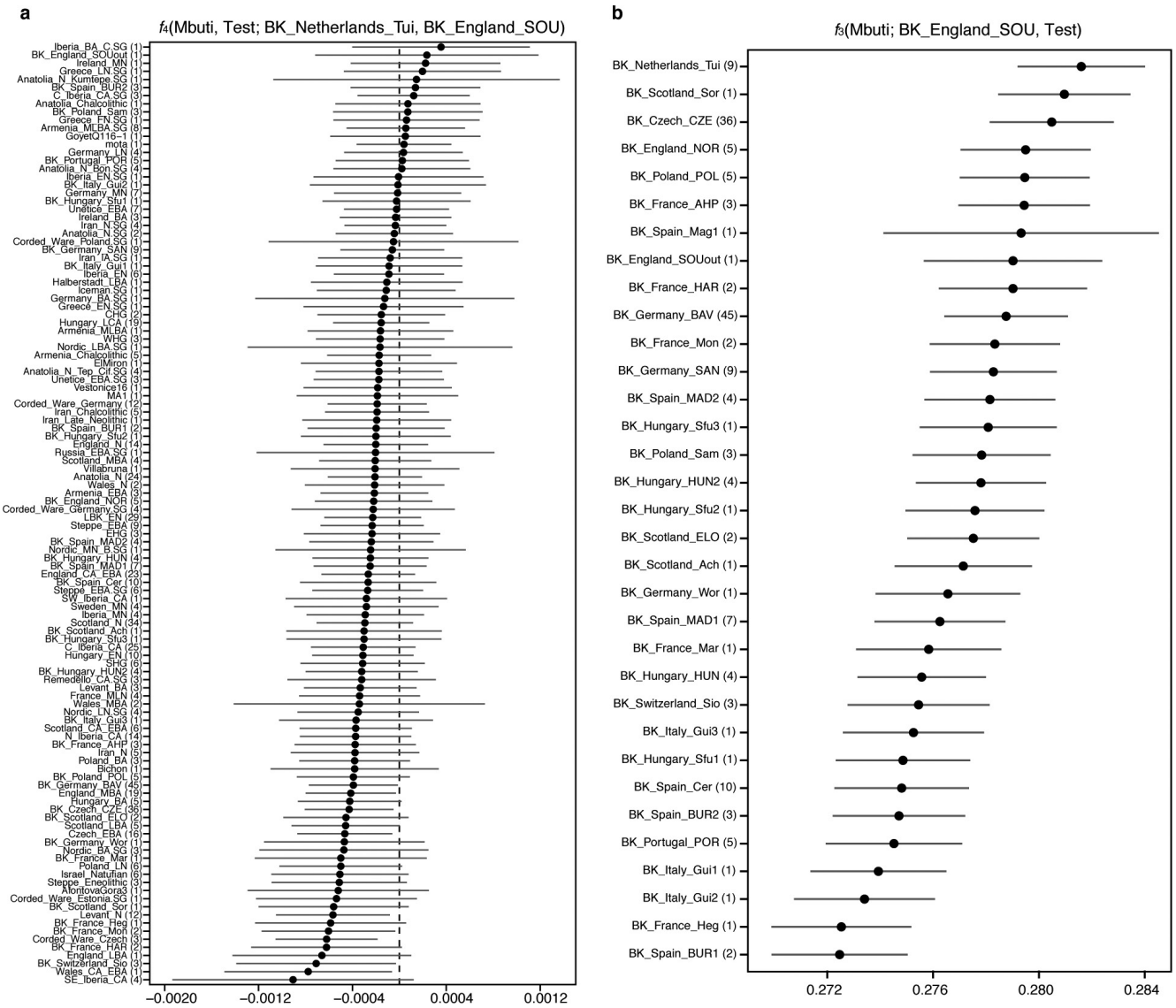

Extended Data Figure 6 | Genetic affinity between Beaker-complex-associated individuals from southern England and the Netherlands. **a**, *f*-statistics of the form f_4(Mbuti, test; BK_Netherlands_Tui, BK_England_SOU). Negative values indicate that test population is closer to BK_Netherlands_Tui than to BK_England_SOU; positive values indicate that the test population is closer to BK_England_SOU than to BK_Netherlands_Tui. Error bars represent ± 3 standard errors. **b**, Outgroup f_3-statistics of the form f_3(Mbuti; BK_England_SOU, test) measuring shared genetic drift between BK_England_SOU and other Beaker-complex-associated groups. Error bars represent ± 1 standard errors. Number of individuals for each group is given in parentheses. BK_Netherlands_Tui, Beaker-complex-associated individuals from De Tuithoorn (Oostwoud, the Netherlands); BK_England_SOU, Beaker-complex-associated individuals from southern England. See Supplementary Table 1 for individuals associated with each population label.

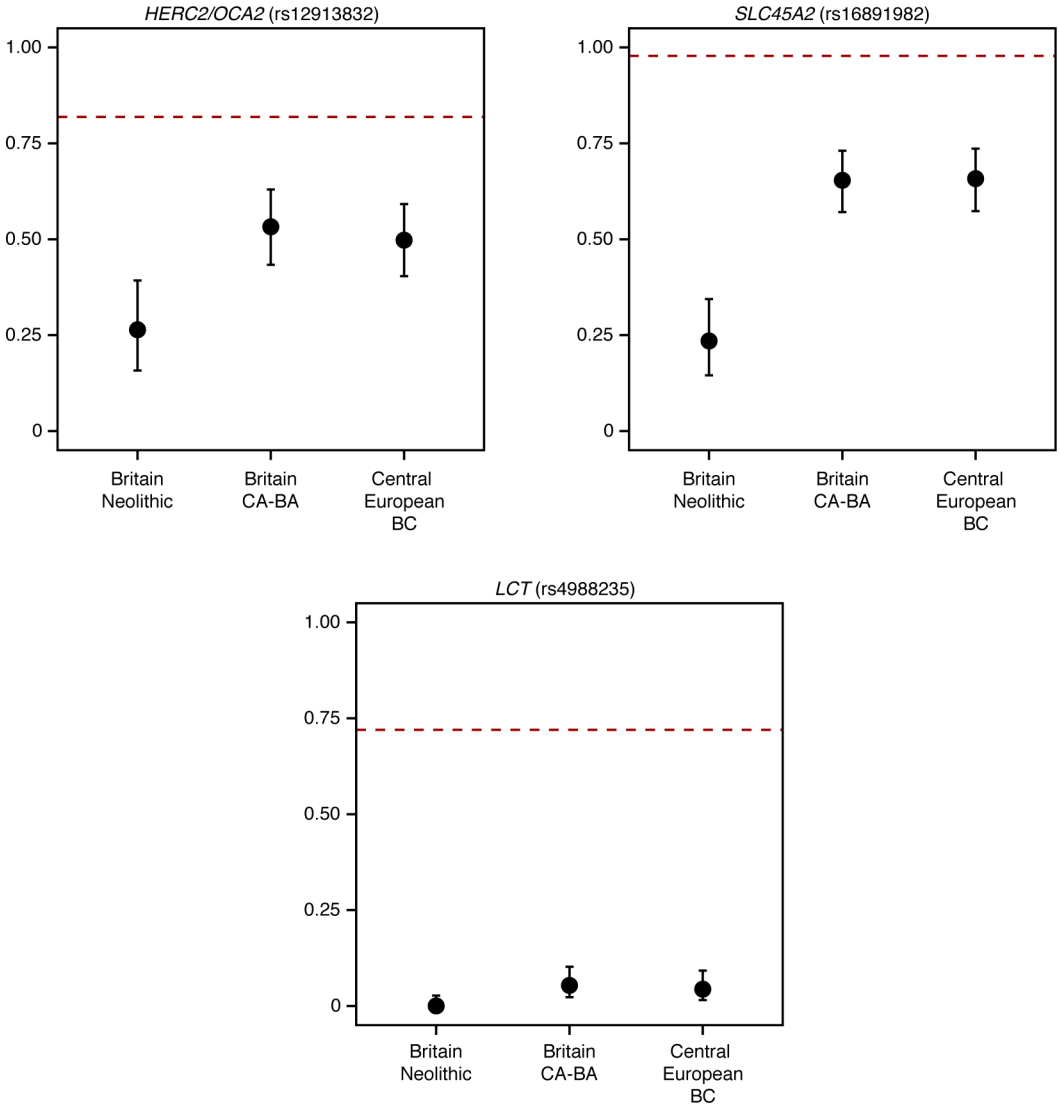

Extended Data Figure 7 | Derived allele frequencies at three SNPs of functional importance. Error bars represent 1.9-log-likelihood support interval. The red dashed lines show allele frequencies in the 1000 Genomes Project (http://www.internationalgenome.org/) 'GBR' population (present-day people from Great Britain). Sample sizes are 50, 98 and 117 for Britain Neolithic, Britain Copper Age and Bronze Age, and central European Beaker-complex-associated individuals, respectively. BC, Beaker complex; CA, Copper Age; and BA, Bronze Age.

Extended Data Table 1 | Sites from outside Britain with new genome-wide data reported in this study

Site	N	Approx. date range (BC)	Country
Brandysek	12	2900–2200	Czech Republic
Kněževes	2	2500–1900	Czech Republic
Lochenice	1	2500–1900	Czech Republic
Lovosice II	1	2500–1900	Czech Republic
Moravská Nová Ves	4	2300–1900	Czech Republic
Prague 5 - Malá Ohrada	1	2500–2200	Czech Republic
Prague 5, Jinonice	14	2200–1700	Czech Republic
Prague 8, Kobylisy, Ke Stírce Street	12	2500–1900	Czech Republic
Radovesice	13	2500–2200	Czech Republic
Velké Přílepy	3	2500–1900	Czech Republic
Clos de Roque, Saint Maximin-la-Sainte-Baume	3	4700–4500	France
Collet Redon, La Couronne-Martigues	1	3500–3100	France
Hégenheim Necropole, Haut-Rhin	1	2800–2500	France
La Fare, Forcalquier	1	2500–2200	France
Marlens, Sur les Barmes, Haute-Savoie	1	2500–2100	France
Mondelange, PAC de la Sente, Moselle	2	2400–1900	France
Rouffach, Haut-Rhin	1	2300–2100	France
Sierentz, Les Villas d'Aurele, Haut-Rhin	2	2600–2300	France
Villard, Lauzet-Ubaye	2	2200–1900	France
Alburg-Lerchenhaid, Spedition Häring, Bavaria	13	2500–2100	Germany
Augsburg Sportgelände, Augsburg, Bavaria	6	2500–2000	Germany
Hugo-Eckener-Straße, Augsburg, Bavaria	3	2500–2000	Germany
Irlbach, County of Straubing-Bogen, Bavaria	17	2500–2000	Germany
Künzing-Bruck, Lkr. Deggendorf, Bavaria	3	2500–2000	Germany
Landau an der Isar, Bavaria	5	2500–2000	Germany
Manching-Oberstimm, Bavaria	2	2500–2000	Germany
Osterhofen-Altenmarkt, Bavaria	4	2600–2000	Germany
Unterer Talweg 58-62, Augsburg, Bavaria	2	2500–2200	Germany
Unterer Talweg 85, Augsburg, Bavaria	1	2400–2100	Germany
Weichering, Bavaria	4	2500–2000	Germany
Worms-Herrnsheim, Rhineland-Palatinate	1	2500–2000	Germany
Budakalász, Csajerszke (M0 Site 12)	2	2600–2200	Hungary
Budapest-Békásmegyer	3	2500–2100	Hungary
Mezőcsát-Hörcsögös	4	3400–3000	Hungary
Szigetszentmiklós-Üdülősor	4	2500–2200	Hungary
Szigetszentmiklós,Felső Ürge-hegyi dűlő	6	2500–2200	Hungary
Pergole 2, Partanna, Sicily	3	2500–1900	Italy
Via Guidorossi, Parma, Emilia Romagna	3	2200–1900	Italy
Dzielnica	1	2300–2000	Poland
Iwiny	1	2300–2000	Poland
Jordanów Śląski	1	2300–2200	Poland
Kornice	4	2500–2100	Poland
Racibórz-Stara Wieś	1	2300–2000	Poland
Samborzec	3	2500–2100	Poland
Strachów	1	2000–1800	Poland
Żerniki Wielkie	1	2300–2100	Poland
Bolores, Estremadura	1	2800–2600	Portugal
Cova da Moura, Torres Vedras	1	2300–2100	Portugal
Galeria da Cisterna, Almonda	2	2500–2200	Portugal
Verdelha dos Ruivos, District of Lisbon	3	2700–2300	Portugal
Arroyal I, Burgos	5	2600–2200	Spain
Camino de las Yeseras, Madrid	14	2800–1700	Spain
Camino del Molino, Caravaca, Murcia	4	2900–2100	Spain
Humanejos, Madrid	11	2900–2000	Spain
La Magdalena, Madrid	3	2500–2000	Spain
Paris Street, Cerdanyola, Barcelona	10	2900–2300	Spain
Virgazal, Tablada de Rudrón, Burgos	1	2300–2000	Spain
Sion-Petit-Chasseur, Dolmen XI	3	2500–2000	Switzerland
De Tuithoorn, Oostwoud, Noord-Holland	11	2600–1600	The Netherlands

Extended Data Table 2 | Sites from Britain with new genome-wide data reported in this study

Site	N	Approx. date range (BC)	Country
Abingdon Spring Road cemetery, Oxfordshire, England	1	2500–2200	Great Britain
Amesbury Down, Wiltshire, England	13	2500–1300	Great Britain
Banbury Lane, Northamptonshire, England	3	3400–3100	Great Britain
Barrow Hills, Radley, Oxfordshire, England	1	2300–1800	Great Britain
Barton Stacey, Hampshire, England	1	2200–2000	Great Britain
Baston and Langtoft, South Lincolnshire, England	2	1700–1600	Great Britain
Biddenham Loop, Bedfordshire, England	9	1600–1300	Great Britain
Boscombe Airfield, Wiltshire, England	1	1800–1600	Great Britain
Canada Farm, Sixpenny Handley, Dorset, England	2	2500–2300	Great Britain
Carsington Pasture Cave, Derbyshire, England	2	3700–2000	Great Britain
Central Flying School, Upavon, Wiltshire, England	1	2500–1800	Great Britain
Cissbury Flint Mine, Worthing, West Sussex, England	1	3600–3400	Great Britain
Clay Farm, Cambridgeshire, England	2	1400–1300	Great Britain
Dairy Farm, Willington, England	1	2300–1900	Great Britain
Ditchling Road, Brighton, Sussex, England	1	2500–1900	Great Britain
Eton Rowing Course, Buckinghamshire, England	2	3600–2900	Great Britain
Flying School, Netheravon, Wiltshire, England	2	2500–1800	Great Britain
Fussell's Lodge, Salisbury, Wiltshire, England	2	3800–3600	Great Britain
Lesser Kelco Cave, Giggleswick Scar, North Yorkshire, England	1	3700–3500	Great Britain
Hasting Hill, Sunderland, Tyne and Wear, England	2	2500–1800	Great Britain
Hexham Golf Course, Northumberland, England	1	2000–1800	Great Britain
Low Hauxley, Northumberland, England	2	2100–1600	Great Britain
Melton Quarry, East Riding of Yorkshire, England	1	1900–1700	Great Britain
Neale's Cave, Paington, Devon, England	1	2000–1600	Great Britain
Nr. Ablington, Figheldean, England	1	2500–1800	Great Britain
Nr. Millbarrow, Wiltshire, England	1	3600–3400	Great Britain
Over Narrows, Needingworth Quarry, England	5	2200–1300	Great Britain
Porton Down, Wiltshire, England	2	2500–1900	Great Britain
Raven Scar Cave, Ingleton, North Yorkshire, England	1	1100–900	Great Britain
Reaverhill, Barrasford, Northumberland, England	1	2100–2000	Great Britain
River Thames, Mortlake/Syon Reach, London, England	2	2500–1700	Great Britain
Staxton Beacon, Staxton, England	1	2400–1600	Great Britain
Summerhill,Blaydon, Tyne and Wear, England	1	1900–1700	Great Britain
East Kent Access (Phase II), Thanet, Kent, England	4	2100–1700	Great Britain
Totty Pot, Cheddar, Somerset, England	1	2800–2500	Great Britain
Trumpington Meadows, Cambridge, England	2	2200–2000	Great Britain
Turners Yard, Fordham, Cambridgeshire, England	1	1700–1500	Great Britain
Upper Swell, Chipping Norton, Gloucestershire, England	1	4000–3300	Great Britain
Waterhall Farm, Chippenham, Cambridgeshire, England	1	2000–1700	Great Britain
West Deeping, Lincolnshire, England	1	2300–2000	Great Britain
Whitehawk, Brighton, Sussex, England	1	3700–3400	Great Britain
Wick Barrow, Stogursey, Somerset, England	1	2400–2000	Great Britain
Wilsford Down, Wilsford-cum-Lake, Wiltshire, England	2	2400–2000	Great Britain
Windmill Fields, Stockton-on-Tees, North Yorkshire,England	4	2300–2000	Great Britain
Yarnton, Oxfordshire, England	4	2500–1900	Great Britain
Aberdour Road, Dunfermline, Fife, Scotland	1	2000–1800	Great Britain
Achavanich, Wick, Highland, Scotland	1	2500–2100	Great Britain
Boatbridge Quarry, Thankerton, Scotland	1	2400–2100	Great Britain
Clachaig, Arran, North Ayrshire, Scotland	1	3500–3400	Great Britain
Covesea Cave 2, Moray, Scotland	3	2100–800	Great Britain
Covesea Caves, Moray, Scotland	2	1000–800	Great Britain
Distillery Cave, Oban, Argyll and Bute, Scotland	3	3800–3400	Great Britain
Doune, Perth and Kinross, Scotland	1	1800–1600	Great Britain
Dryburn Bridge, East Lothian, Scotland	2	2300–1900	Great Britain
Eweford Cottages, East Lothian, Scotland	1	2100–1900	Great Britain
Holm of Papa Westray North, Orkney, Scotland	4	3500–3100	Great Britain
Isbister, Orkney, Scotland	10	3300–2300	Great Britain
Leith, Merrilees Close, City of Edinburgh, Scotland	2	1600–1500	Great Britain
Longniddry, Evergreen House, Coast Road, East Lothian, Scotlan	3	1500–1300	Great Britain
Longniddry, Grainfoot, East Lothian, Scotland	1	1300–1000	Great Britain
Macarthur Cave, Oban, Argyll and Bute, Scotland	1	4000–3800	Great Britain
Pabay Mor, Lewis, Western Isles, Scotland	1	1400–1300	Great Britain
Point of Cott, Orkney, Scotland	2	3700–3100	Great Britain
Quoyness, Orkney, Scotland	1	3100–2900	Great Britain
Raschoille Cave, Oban, Argyll and Bute, Scotland	9	4000–2900	Great Britain
Sorisdale, Coll, Argyll and Bute, Scotland	1	2500–2100	Great Britain
Stenchme, Lop Ness, Orkney, Scotland	1	2000–1500	Great Britain
Thurston Mains, Innerwick, East Lothian, Scotland	1	2300–2000	Great Britain
Tulach an t'Sionnach, Highland, Scotland	1	3700–3500	Great Britain
Tulloch of Assery A, Highland, Scotland	1	3700–3400	Great Britain
Tulloch of Assery B, Highland, Scotland	1	3800–3600	Great Britain
Unstan, Orkney, Scotland	1	3400–3100	Great Britain
Culver Hole Cave, Port Eynon, West Glamorgan, Wales	1	1600–800	Great Britain
Great Orme Mines, Llandudno, North Wales	1	1700–1600	Great Britain
North Face Cave, Llandudno, North Wales	1	1400–1200	Great Britain
Rhos Ddigre, Llanarmon-yn-Îâl, Denbighshire, Wales	1	3100–2900	Great Britain
Tinkinswood, Cardiff, Glamorgan, Wales	1	3800–3600	Great Britain

Extended Data Table 3 | 111 newly reported radiocarbon dates

Sample	Date	Location	Country
I5024	2278–2032 calBC (3740±35 BP, Poz-84460)	Kněževes	Czech Republic
I4946	2296–2146 calBC (3805±20 BP, PSUAMS-2801)	Prague 5, Jinonice, Butovická Street	Czech Republic
I4895	2273–2047 calBC (3750±20 BP, PSUAMS-2852)	Prague 5, Jinonice, Butovická Street	Czech Republic
I4896	2288–2142 calBC (3785±20 BP, PSUAMS-2853)	Prague 5, Jinonice, Butovická Street	Czech Republic
I4884	1882–1745 calBC (3480±20 BP, PSUAMS-2842)	Prague 8, Kobylisy, Ke Stirce Street	Czech Republic
I4885	2289–2143 calBC (3790±20 BP, PSUAMS-2843)	Prague 8, Kobylisy, Ke Stirce Street	Czech Republic
I4886	2205–2042 calBC (3740±20 BP, PSUAMS-2844)	Prague 8, Kobylisy, Ke Stirce Street	Czech Republic
I4887	2201–2039 calBC (3730±20 BP, PSUAMS-2845)	Prague 8, Kobylisy, Ke Stirce Street	Czech Republic
I4888	2190–2029 calBC (3700±20 BP, PSUAMS-2846)	Prague 8, Kobylisy, Ke Stirce Street	Czech Republic
I4889	2281–2062 calBC (3765±20 BP, PSUAMS-2847)	Prague 8, Kobylisy, Ke Stirce Street	Czech Republic
I4891	2281–2062 calBC (3765±20 BP, PSUAMS-2848)	Prague 8, Kobylisy, Ke Stirce Street	Czech Republic
I4892	1881–1701 calBC (3475±20 BP, PSUAMS-2849)	Prague 8, Kobylisy, Ke Stirce Street	Czech Republic
I4893	4449–4348 calBC (5550±20 BP, PSUAMS-2850)	Prague 8, Kobylisy, Ke Stirce Street	Czech Republic
I4894	4488–4368 calBC (5610±20 BP, PSUAMS-2851)	Prague 8, Kobylisy, Ke Stirce Street	Czech Republic
I4945	2291–2144 calBC (3795±20 BP, PSUAMS-2854)	Prague 8, Kobylisy, Ke Stirce Street	Czech Republic
I4305	4825–4616 calBC (5860±35 BP, PSUAMS-2225)	Clos de Roque, Saint Maximin-la-Sainte-Baume	France
I4304	4787–4589 calBC (5830±35 BP, PSUAMS-2226)	Clos de Roque, Saint Maximin-la-Sainte-Baume	France
I4303	4778–4586 calBC (5820±30 BP, PSUAMS-2260)	Clos de Roque, Saint Maximin-la-Sainte-Baume	France
I1392	2833–2475 calBC (4047±29 BP, MAMS-25935)	Hégenheim Necropole, Haut-Rhin	France
I3875	2133–1946 calBC (3655±25 BP, PSUAMS-1834)	Villard, Lauzet-Ubaye	France
I3874	2200–2035 calBC (3725±25 BP, PSUAMS-1835)	Villard, Lauzet-Ubaye	France
I3593	2397–2145 calBC (3817±26 BP, BRAMS-1215)	Alburg-Lerchenhaid, Spedition Häring, Stkr. Straubing, Bavaria	Germany
I3590	2335–2140 calBC (3802±26 BP, BRAMS-1217)	Alburg-Lerchenhaid, Spedition Häring, Stkr. Straubing, Bavaria	Germany
I3592	2457–2203 calBC (3844±33 BP, BRAMS-1218)	Alburg-Lerchenhaid, Spedition Häring, Stkr. Straubing, Bavaria	Germany
I5017	2460–2206 calBC (3855±35 BP, Poz-84458)	Augsburg Sportgelände, Augsburg, Bavaria	Germany
I4250	2433–2149 calBC (3825±26 BP, BRAMS-1219)	Irlbach, County of Straubing-Bogen, Bavaria	Germany
I5021	2571–2341 calBC (3955±35 BP, Poz-84553)	Osterhofen-Altenmarkt, Bavaria	Germany
E09537_d	2471–2298 calBC (3909±29 BP, MAMS-29074)	Unterer Talweg 58-62, Augsburg, Bavaria	Germany
E09538	2464–2210 calBC (3870±30 BP, MAMS-29075)	Unterer Talweg 58-62, Augsburg, Bavaria	Germany
I5385	2455–2147 calBC (3827±33 BP, SUERC-71005)	Achavanich, Wick, Highland, Scotland	Great Britain
I2457	2199–2030 calBC (3717±28 BP, SUERC-69975)	Amesbury Down, Wiltshire, England	Great Britain
I2416	2455–2151 calBC (3830±30 BP, Beta-432804)	Amesbury Down, Wiltshire, England	Great Britain
I2596	2273–2034 calBC (3739±30 BP, NZA-32484)	Amesbury Down, Wiltshire, England	Great Britain
I2566	2204–2035 calBC (3734±25 BP, NZA-32490)	Amesbury Down, Wiltshire, England	Great Britain
I2598	2135–1953 calBC (3664±30 BP, NZA-32494)	Amesbury Down, Wiltshire, England	Great Britain
I2418	2455–2200 calBC (3836±25 BP, NZA-32788)	Amesbury Down, Wiltshire, England	Great Britain
I2565	2457–2147 calBC (3829±38 BP, OxA-13562)	Amesbury Down, Wiltshire, England	Great Britain
I2457	2467–2290 calBC (3890±30 BP, SUERC-36210)	Amesbury Down, Wiltshire, England	Great Britain
I2460	2022–1827 calBC (3575±27 BP, SUERC-53041)	Amesbury Down, Wiltshire, England	Great Britain
I2459	2455–2150 calBC (3829±30 BP, SUERC-54823)	Amesbury Down, Wiltshire, England	Great Britain
I5373	2194–1980 calBC (3694±25 BP, BRAMS-1230)	Carsington Pasture Cave, Brassington, Derbyshire, England	Great Britain
I2988	3516–3361 calBC (4645±29 BP, SUERC-68711)	Clachaig, Arran, North Ayrshire, Scotland	Great Britain
I2860	969–815 calBC (2738±29 BP, SUERC-68715)	Covesea Cave 2, Moray, Scotland	Great Britain
I2861	976–828 calBC (2757±29 BP, SUERC-68716)	Covesea Cave 2, Moray, Scotland	Great Britain
I3132	2118–1887 calBC (3614±33 BP, SUERC-69070)	Covesea Cave 2, Moray, Scotland	Great Britain
I3130	977–829 calBC (2758±29 BP, SUERC-68713)	Covesea Caves, Moray, Scotland	Great Britain
I2859	910–809 calBC (2714±29 BP, SUERC-68714)	Covesea Caves, Moray, Scotland	Great Britain
I2452	2198–1980 calBC (3700±30 BP, Beta-444979)	Dairy Farm, Willington, England	Great Britain
I2452	2276–2029 calBC (3735±35 BP, Poz-83405)	Dairy Farm, Willington, England	Great Britain
I2659	3761–3643 calBC (4914±27 BP, SUERC-68702)	Distillery Cave, Oban, Argyll and Bute, Scotland	Great Britain
I2660	3513–3352 calBC (4631±29 BP, SUERC-68703)	Distillery Cave, Oban, Argyll and Bute, Scotland	Great Britain
I2691	3700–3639 calBC (4881±25 BP, SUERC-68704)	Distillery Cave, Oban, Argyll and Bute, Scotland	Great Britain
I6774	2287–2044 calBC (3760±30 BP, SUERC-74755)	Ditchling Road, Brighton, Sussex, England	Great Britain
I2605	3631–3372 calBC (4710±35 BP, Poz-83483)	Eton Rowing Course, Buckinghamshire, England	Great Britain
I1775	1730–1532 calBC (3344±27 BP, OxA-14308)	Great Orme, Llandudno, North Wales	Great Britain
I2574	1414–1227 calBC (3065±36 BP, SUERC-62072)	Great Orme, Llandudno, North Wales	Great Britain
I2612	2464–2208 calBC (3865±35 BP, Poz-83492)	Hasting Hill, Sunderland, Tyne and Wear, England	Great Britain
I2609	2022–1771 calBC (3560±40 BP, Poz-83423)	Hexham Golf Course, Northumberland, England	Great Britain
I2636	3519–3361 calBC (4651±33 BP, SUERC-68640)	Holm of Papa Westray North, Orkney, Scotland	Great Britain
I2637	3629–3370 calBC (4697±33 BP, SUERC-68641)	Holm of Papa Westray North, Orkney, Scotland	Great Britain
I2650	3638–3380 calBC (4754±36 BP, SUERC-68642)	Holm of Papa Westray North, Orkney, Scotland	Great Britain
I2651	3360–3098 calBC (4525±36 BP, SUERC-68643)	Holm of Papa Westray North, Orkney, Scotland	Great Britain
I2630	2580–2463 calBC (3999±32 BP, SUERC-68632)	Isbister, Orkney, Scotland	Great Britain
I2932	2570–2347 calBC (3962±29 BP, SUERC-68721)	Isbister, Orkney, Scotland	Great Britain
I2933	3010–2885 calBC (4309±29 BP, SUERC-68722)	Isbister, Orkney, Scotland	Great Britain
I2935	3335–3011 calBC (4451±29 BP, SUERC-68723)	Isbister, Orkney, Scotland	Great Britain
I3085	3338–3026 calBC (4471±29 BP, SUERC-68724)	Isbister, Orkney, Scotland	Great Britain
I2978	3335–3023 calBC (4464±29 BP, SUERC-68725)	Isbister, Orkney, Scotland	Great Britain
I2979	3333–2941 calBC (4447±29 BP, SUERC-68726)	Isbister, Orkney, Scotland	Great Britain
I2934	3338–3022 calBC (4466±33 BP, SUERC-69071)	Isbister, Orkney, Scotland	Great Britain
I2977	3008–2763 calBC (4275±33 BP, SUERC-69072)	Isbister, Orkney, Scotland	Great Britain
I2657	3951–3780 calBC (5052±30 BP, SUERC-68701)	Macarthur Cave, Oban, Argyll and Bute, Scotland	Great Britain
I5441	1938–1744 calBC (3512±37 BP, OxA-16522)	Neale's Cave, Paington, Devon, England	Great Britain
I4949	3629–3376 calBC (4715±20 BP, PSUAMS-2513)	Nr. Millbarrow, Winterbourne Monkton, Wiltshire, England	Great Britain
I2980	3360–3101 calBC (4530±33 BP, SUERC-69073)	Point of Cott, Orkney, Scotland	Great Britain
I2796	3705–3535 calBC (4856±33 BP, SUERC-69074)	Point of Cott, Orkney, Scotland	Great Britain
I2631	3097–2906 calBC (4384±36 BP, SUERC-68633)	Quoyness, Orkney, Scotland	Great Britain
I3135	3640–3383 calBC (4770±30 BP, PSUAMS-2068)	Raschoille Cave, Oban, Argyll and Bute, Scotland	Great Britain
I3136	3520–3365 calBC (4665±30 BP, PSUAMS-2069)	Raschoille Cave, Oban, Argyll and Bute, Scotland	Great Britain
I3133	3631–3377 calBC (4725±20 BP, PSUAMS-2154)	Raschoille Cave, Oban, Argyll and Bute, Scotland	Great Britain
I3134	3633–3377 calBC (4730±25 BP, PSUAMS-2155)	Raschoille Cave, Oban, Argyll and Bute, Scotland	Great Britain
I3138	3263–2923 calBC (4415±25 BP, PSUAMS-2156)	Raschoille Cave, Oban, Argyll and Bute, Scotland	Great Britain
I2610	1935–1745 calBC (3515±35 BP, Poz-83498)	Summerhill, Blaydon, Tyne and Wear, England	Great Britain
I2634	3703–3534 calBC (4851±34 BP, SUERC-68638)	Tulach an t'Sionnach, Highland, Scotland	Great Britain
I2635	3652–3389 calBC (4796±37 BP, SUERC-68639)	Tulloch of Assery A, Highland, Scotland	Great Britain
I2633	3765–3641 calBC (4911±32 BP, SUERC-68634)	Tulloch of Assery B, Highland, Scotland	Great Britain
I2453	2288–2040 calBC (3760±35 BP, Poz-83404)	West Deeping, Lincolnshire, England	Great Britain
I2445	2136–1929 calBC (3650±35 BP, Poz-83407)	Yarnton, Oxfordshire, England	Great Britain
I2447	2115–1910 calBC (3625±25 BP, PSUAMS-2336)	Yarnton, Oxfordshire, England	Great Britain
I2786	2458–2205 calBC (3850±35 BP, Poz-83639)	Szigetszentmiklós-Felső-Ürge hegyi dűlő	Hungary
I2787	2457–2201 calBC (3840±35 BP, Poz-83640)	Szigetszentmiklós-Felső-Ürge hegyi dűlő	Hungary
I2741	2457–2153 calBC (3835±35 BP, Poz-83641)	Szigetszentmiklós-Felső-Ürge hegyi dűlő	Hungary
I6531	2286–2038 calBC (3755±35 BP, Poz-86947)	Dzielnica	Poland
I6579	2335–2046 calBC (3780±35 BP, Poz-75954)	Iwiny	Poland
I6534	2456–2149 calBC (3830±35 BP, Poz-75936)	Kornice	Poland
I6582	2343–2057 calBC (3790±35 BP, Poz-75951)	Kornice	Poland
I4251	2431–2150 calBC (3825±25 BP, PSUAMS-2321)	Samborzec 1	Poland
I4252	2285–2138 calBC (3780±20 BP, PSUAMS-2338)	Samborzec 1	Poland
I4253	2456–2207 calBC (3850±20 BP, PSUAMS-2339)	Samborzec 1	Poland
I6538	2008–1765 calBC (3545±35 BP, Poz-86950)	Strachów	Poland
I6583	2289–2050 calBC (3770±30 BP, Poz-65207)	Zerniki Wielkie	Poland
I4229	2288–2134 calBC (3775±25 BP, PSUAMS-1750)	Cova da Moura	Portugal
I0462	2566–2345 calBC (3950±26 BP, MAMS-25936)	Arroyal I, Burgos	Spain
I4247	2464–2210 calBC (3870±30 BP, PSUAMS-2120)	Camino de las Yeseras, Madrid	Spain
I4245	2460–2291 calBC (3875±20 BP, PSUAMS-2320)	Camino de las Yeseras, Madrid	Spain
I0257	2572–2348 calBC (3965±29 BP, MAMS-25937)	Paris Street, Cerdanyola, Barcelona	Spain
I0825	2474–2298 calBC (3915±29 BP, MAMS-25939)	Paris Street, Cerdanyola, Barcelona	Spain
I0826	2834–2482 calBC (4051±28 BP, MAMS-25940)	Paris Street, Cerdanyola, Barcelona	Spain
I4068	2131–1951 calBC (3655±20 BP, PSUAMS-2318)	De Tuithoorn, Oostwoud, Noord-Holland	The Netherlands
I4076	1882–1750 calBC (3490±20 BP, PSUAMS-2319)	De Tuithoorn, Oostwoud, Noord-Holland	The Netherlands
I4075	2118–1937 calBC (3635±20 BP, PSUAMS-2337)	De Tuithoorn, Oostwoud, Noord-Holland	The Netherlands